Realization of a Localized Surface Plasmon Resonance Gas Sensor, Based on Ag nanoparticles

Sh. Khalili Fard[1], S. Darbari[1*], V. Ahmadi[1]

***Abstract*—— Here, the response of localized surface plasmon resonance (LSPR) gas sensor has been investigated, which consists of Ag nanoparticles on glass. Output characteristic of the proposed LSPR gas sensor are investigated by exposure of different concentrations of N_2 to the structure (0-250 ppm). Ag nanoparticles are synthesized chemical method, which has been optimized in order to achieve the best detection sensitivity in the output behaviour of the sensor. It is shown that the best output response is achieved for Ag nanoparticles with the diameter of about 30 nm and LSPR peak at wavelength of about 415 nm. Physical adsorption of N_2 molecules on Ag nanoparticles increases the refractive index of the enclosing environment, and leads to a red-shift in the wavelength of localized surface plasmons. It is illustrated here that the shift of the LSPR spectrum is sensitive to the concentration of exposed nitrogen, with a sensitivity of about 0.56 nm versus gas concentration variation of about 100 ppm. Our experimental investigations are in agreement with the simulation results, relating to the similar structure.**

***Index Terms*—Localized surface plasmon resonance; Ag nanoparticles; reduced graphene oxide; gas sensor; sensitivity;**

I. Introduction

THIS urface plasmon resonance (SPR) is an optical property of metallic structures that has widely attracted research activities recently [1]. SPR is the resonant oscillation of conduction electrons at the interface between two materials with opposite sign of permittivity, and can be excited by the electromagnetic field of incident light [1, 2]. Surface plasmons are emerging in many application fields, including biomedical, environment protection and chemical sensing [3, 4]. In a metallic particle, the electrons are confined in three dimensions, and oscillation of the electron induce an electric field around the particle [5]. When the size of metallic particle is reduced to a few nanometers, the optical properties of SPs will be completely different from the bulk material [2, 5, 6]. In this case, the resonance of SPs will be localized around the particle. Recently, localized surface
plasmon resonance (LSPR), associated with metal nanostructures, has created new opportunities for detection of molecular interactions [7], and different sensing applications owing to high sensitivity to the environmental variations [8, 9].

In this work, Ag nanoparticles (Ag NPs) on glass were used to realize LSPR gas sensor. Ag NPs, with a sharp peak at about 415nm, and simple synthesis, are entitled as a promising sensing element for LSPR gas sensors. First, we investigate the change of LSPR spectrum, as a consequence of N_2 exposure, with different concentrations. Then, taking advantage of Mie theory [5, 10], we have attributed the observed shift in the LSPR spectrum to the change in refractive index of enclosing environment of the nanoparticles [2, 6, 7]. Then, we show that the achieved experimental data are in acceptable agreement with the discussed model.

II. Materials and Methods

In this study, Ag nanoparticles are prepared by chemical synthesis method [11, 12]. In this method, sodium borohydride ($NaBH_4$) was used as a reducing agent to reduce the ionic silver and to stabilize the synthesized silver nanoparticles. The related chemical reaction is shown as [13]:

$$AgNO_3 + NaBH_4 \rightarrow Ag + \frac{1}{2}H_2 + \frac{1}{2}B_2H_6 + NaNO_3$$

Different volumes of 0.001M silver nitrate (2, 5, 7, 10 ml $AgNO_3$) is added (about 1 drop per second) to 30 ml of 0.002M $NaBH_4$ solution, which have been cooled in an ice containing beaker. The reaction mixture is stirred simultaneously, at a rate of about 600rpm on a magnetic stirrer [11]. Different volumes of $AgNO_3$ have been utilized to obtain the optimized median size for the synthesized Ag nanoparticles. Then, the synthesized nanoparticles liquid is dispersed on a pre-cleaned glass substrate and was dried in the oven at 80°C.

In order to investigate the output behaviour of the fabricated structure as a LSPR gas sensor, optical property of the sample is investigated while a controlled concentration of N_2 gas is introduced into the chamber. The reason for choosing this gas, was that only physical adsorption occurs for elemental molecules and hence sensitivity of sensor indicate high sensitivity to compound molecules and vapours. The optical investigation is carried out by UV-Vis spectroscopy, in the range of 200–800nm. A halogen source beam is normally illuminated to the testing sample and the transmitted beam is coupled to a spectrometer successfully. Fig. 1 shows the test set up schematically, in which the surrounding gas molecules determine the refractive index of the media (n_m). In all steps of increasing the concentration of target gas, the absorbance measurements with UV-Vis spectroscopy have done while N_2

Manuscript received June 01, 2016; accepted August 22, 2016

[1] Department of Electrical & Computer Engineering, Tarbiat Modares University, Tehran, Iran. Corresponding author: s.darbari@modares.ac.ir

exposure was applied simultaneously (in all steps, optical measurements were done under gas exposure).

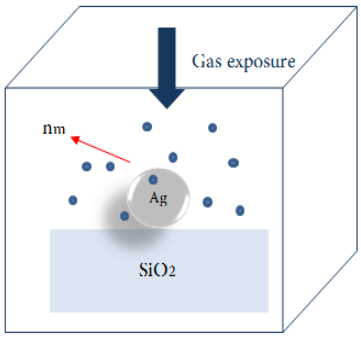

Fig.1: The applied test setup for investigating the fabricated gas sensor. The introduced gas molecules are adsorbed onto the surface of Ag nanoparticles physically and determine the refractive index of the environment (n_m).

III. Experimental Results

To optimize the size of Ag nanoparticles, we have changed the volume of $AgNO_3$ and investigated the LSPR spectrum, accordingly. The optical absorbance spectra of Ag NPs, resulted from 2ml, 5ml, 7ml and 10ml of $AgNO_3$ (1mM), are illustrated in Fig. 2 It can be observed that absorption peak of nanoparticles occurs at about 415nm, which is attributed to LSPR excitement and coincides with previous reports on Ag NPs [11, 12].We have applied nanoparticles resulted from 7ml solution of $AgNO_3$ to fabricate the gas sensor, because of the observed higher intensity of the main LSPR peak at around 415 nm in comparison with samples of 2 ml and 5 ml and the intensity of spectra was higher and favourable for next steps of our researches. Also, it is observable that a broad/second mode peak has been emerged at about 470 nm for the sample with 10ml of $AgNO_3$, which can disturb the sensing functionality of the main peak.

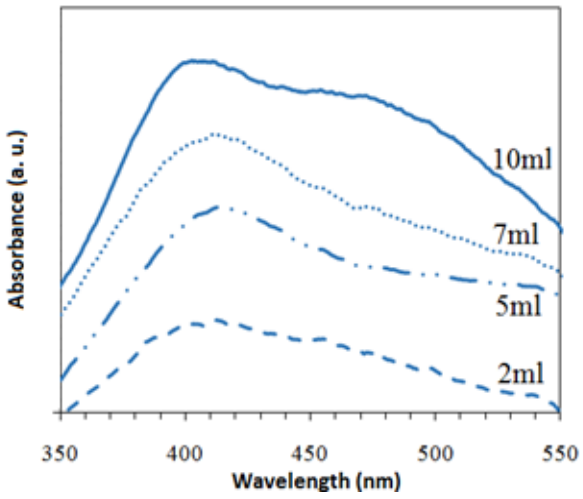

Fig. 2: The absorption spectra of Ag nanoparticles, synthesized by different volumes of $AgNO_3$.

SEM image of the achieved Ag NPs is depicted in Fig3, which indicates an average size of about 30 nm.To investigate the effect of gas exposure on the LSPR spectrum of the sample, we have carried out optical spectroscopy, while the sample is exposed to different concentrations of N_2 (as shown in Fig. 1). As shown in Fig. 1, when the nanoparticle is exposed to low gas concentration, gas molecules physically adsorb on the surface of the particle as the first monolayer.

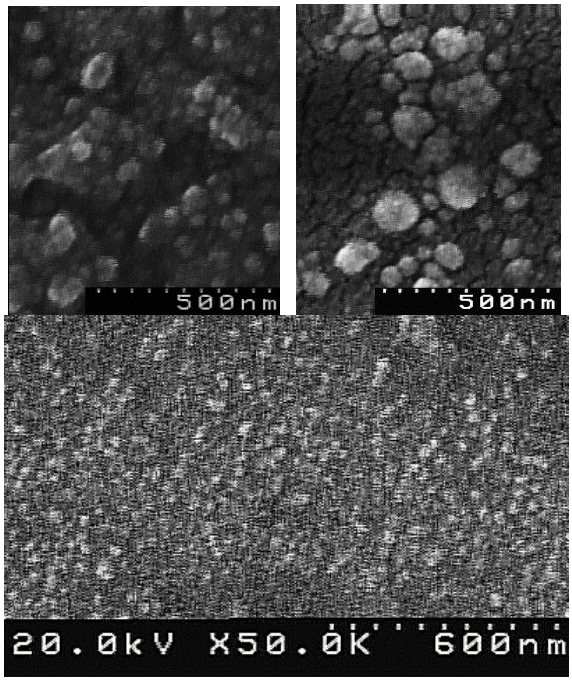

Fig. 3: SEM image of the Ag NPs, using (a) 5ml and (b) 7ml $AgNO_3$.

On the other hand, for higher gas concentrations, surface condensation takes place and multi-layers of gas molecules cover the surface of the nanoparticle. Up to this point, the sensitivity increases as the thickness of the surface condensation layer increases. Increasing the gas concentration leads to increment of the refractive index of the surrounding media (n_m), consequently. Fig. 4 indicates the absorption spectra of the realized LSPR sensor, as a result of different gas concentrations. It is observable that by increasing the introduced gas concentration, a red shift of LSPR peak occurs. The first and the last peak positions, relating to 0 ppm and 250 ppm respectively, are highlighted by arrows, in this figure.

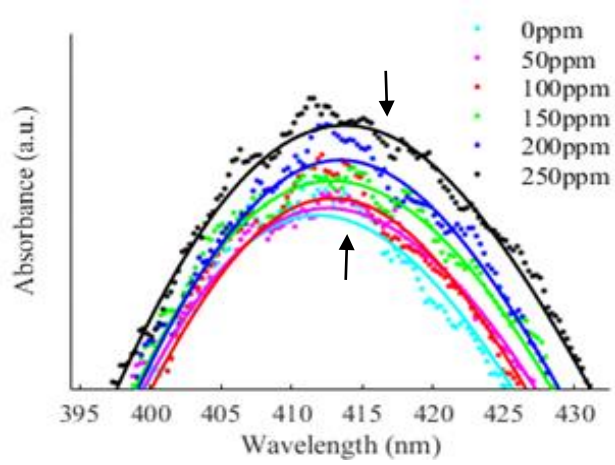

Fig. 4: Absorption spectra of Ag NPs for different gas concentrations (0-250 ppm) [dash lines are experimental data from spectrometer and solid lines are smooth form of these data without probabilistic errors].

Fig.5 indicates the observed variation of LSPR peak in Fig. 4, versus the introduced gas concentration. In this figure λ_{LSPR} is wavelength of LSPR in exposure to gas molecules. It can be observed that there is a nearly linear relationship between LSPR wavelength and

gas concentration. However, it is obvious that LSPR based detection of N_2, requires high-resolution spectrometer which is capable of measuring very small LSPR peak shifts. Here, the resolution of the spectrometer was about 0.001 nm.

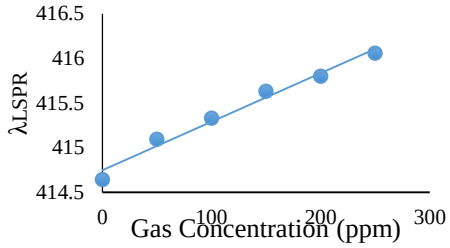

Fig. 5: LSPR shift of the structure vs. N_2 gas concentrations [0 indicate the basic mode without any N_2 gas]

The maximum shift is measured about 1.4 nm versus exposure of about 250 ppm of N_2 (Fig. 5). Thus, the output sensitivity of the realized LSPR gas sensor can be calculated as $S=\Delta\lambda_{LSPR}/\Delta C$, which yields a value of about 0.0056 nm/ppm.

To explain the observed LSPR red shift, when gas molecules are exposed to the sample, we have applied Mie theory [6, 14]. According to this model, it is well established that the peak wavelength of LSPR in metallic nanoparticles is related to refractive index of the environment medium, as equation (1) [6]:

$$\lambda_{LSPR} = \lambda_P\sqrt{(2n_m{}^2 + 1)} \qquad (1)$$

where, λ_{LSPR}, λ_P and n_m are the peak wavelength of LSPR, plasma frequency of metal and refractive index of the environmental media. This relation reveals a red shift in λ_{LSPR}, as a consequence of increasing n_m, which is in accordance with our observed experimental results (Fig. 4, 5). Considering a nearly linear relation between n_m and the introduced gas concentration, Equation 1, also confirms the observed approximately linear behaviour in Fig. 5.

As the last part of this section, we have compared the achieved results with the similar experimental reports. Table 1 summarizes the LSPR shift results of our work beside other reports, which reveals that Ag NPs show a high sensitivity to low concentrations of nitrogen.

TABLE I
. THE LSPR SHIFT OF DIFFERENT AG NP BASED LSPR GAS SENSORS

Structure	Target gas	LSPR shift (Δλ)	Ref.
Ag NP	N_2 250ppm in air	1.4 nm	This work
Ag NP	SF_6 in N_2	0.15 nm	[3]
	CO_2 in N_2	0.17 nm	
Ag NP	N_2 in He	0.058 nm	[8]
	Ar in He	0.048 nm	
Ag NP	n-Octane 10000ppm	2.5 nm	[9]

IV. Simulation Results

To elaborate more on the behaviour of the realized LSPR sensor, we have simulated the structure by FDTD numerical method, using Lumerical software. This algorithm is based on solving Maxwell's equations in time domain. The unit cell of the sensor consists of Ag NPs on SiO_2 substrate, which is displayed in Fig. 6.

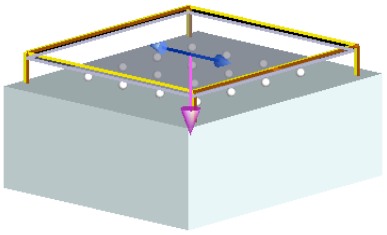

Fig.6: Three-dimensional view of the simulated LSPR sensor structure, consisting of Ag NPs on SiO_2

Input plane wave light with the wavelength range of 200-800 nm was illuminated to the structure in vertically mode. The distance between neighbouring particles is assumed twice their diameter, which coincides with the prepared SEM image (Fig. 3). To investigate the effect of the particle size on the LSPR peak, different radius of Ag particles (15, 20, 24, 26, 28nm) have been investigated, the results of which are presented in Fig. 7. As can be seen in this figure, increasing the size leads to increment of the intensity of LSPR absorption peak. However, further increasing the size (higher than about 30 nm), widens the absorption spectrum which disturbs the sensing behaviour. The refractive index of the surrounding environment is considered 1, equally.

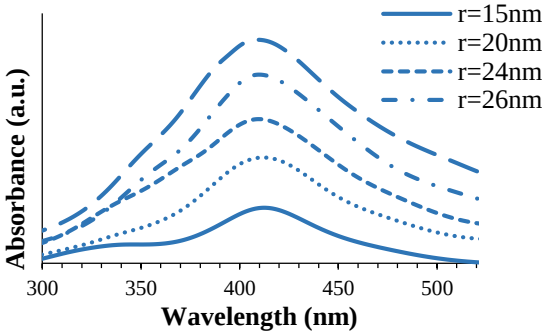

Fig.7: Simulated LSPR absorption spectra for different sizes of Ag NPs

To simulate the effect of refractive index of the surrounding media on the LSPR peak, refractive index of the environment has been changed from 1 to 1.05 in Fig. 8. In this step, the diameter of Ag NPs is approximated equal to 30 nm.

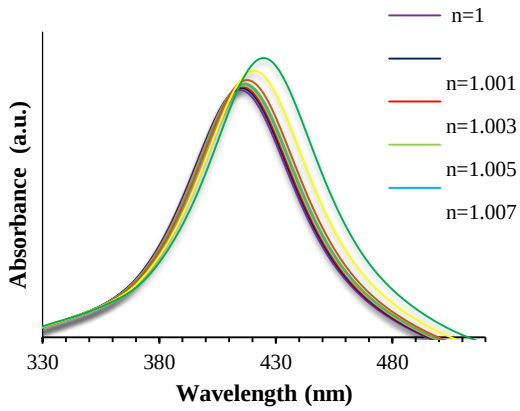

Fig. 8: Simulated LSPR absorption spectra, with different refractive index of the surrounding media. Diameter of Ag NPs is assumed 30 nm

As expected, simulation r`esults in this figure shows that increasing the refractive index of media shifts the resulted LSPR peak to higher wavelengths, similar to our experimental results in Fig. 4.

To compare the achieved experimental and simulation results, we should convert the exerted gas concentration to refractive index of the gas environment. For this purpose, we have applied the well-established relation between the refractive index of a gas environment with the gas pressure (P) and the temperature (T) [15]. So, we obtain $n-1=\mu\frac{P}{T}$, where μ is a constant and is about 810×10^{-9} $(K.Pa^{-1})$ for N_2 [16]. To determine the gas pressure inside the test chamber in our experiments, we have utilized a reference pressure sensor inside the chamber (MPX2202). Regarding the measured pressure values, the exerted refractive index for gas concentrations of 0 ppm (vacuum) to 250 ppm, is estimated to be change from 1 to 1.00025. Therefore, experimental results revealed 1.4 nm shift in λ_{LSPR}, versus changing refractive index by 0.00025, which is equal to increasing the exposed N_2 concentration from 0 to 250 ppm.

Regarding the latter discussion, to correspond the refractive index value in the simulation results, with the exerted experimental conditions, we should consider refractive indices from 1 (0 ppm) to around 1.00025 (250 ppm). It is observable in Fig. 8, that this range of refractive index reveals a LSPR shift of about 1.2 nm, which is in good agreement with the experimental result (1.4 nm). Thus, we can successfully attribute the observed red shift behaviour of the fabricated gas sensor, to increment of the refractive index of the particle's media, after physical absorption of gas molecules on the particles.

V. CONCLUSIONS

In this work, output behaviour of a LSPR gas sensor, based on Ag NPs, has been reported. Ag NPs have been synthesized chemically, with an optimized size of about 30 nm. We have shown that nitrogen exposure leads to a red shift of LSPR peak in the fabricated sensor, with a nearly linear relation between the LSPR peak and nitrogen concentration. An output sensitivity (=$\Delta\lambda/\Delta C$) of about 0.0056 nm/ppm has been measured for Ag nanoparticles in response to N_2 exposure. The achieved results have been explained by Mie theory. Also, we have carried out numerical simulations and showed that the reported experimental results coincide with simulation results quantitatively.

REFERENCES

[1] J. Homola, S. S. Yee, and G. Gauglitz, "Surface plasmon resonance sensors: review," Sensors and Actuators B: Chemical, vol. 54, pp. 3-15, 1999.

[2] K. A. Willets and R. P. Van Duyne, "Localized surface plasmon resonance spectroscopy and sensing," Annu. Rev. Phys. Chem., vol. 58, pp. 267-297, 2007.

[3] T. Ghodselahi, S. Hoornam, M. Vesaghi, B. Ranjbar, A. Azizi, and H. Mobasheri, "Fabrication Localized Surface Plasmon Resonance sensor chip of gold nanoparticles and detection lipase–osmolytes interaction," Applied Surface Science, vol. 314, pp. 138-144, 2014.

[4] L. E. Kreno, J. T. Hupp, and R. P. Van Duyne, "Metal− organic framework thin film for enhanced localized surface plasmon resonance gas sensing," Analytical chemistry, vol. 82, pp. 8042-8046, 2010.

[5] K. M. Mayer and J. H. Hafner, "Localized surface plasmon resonance sensors," Chemical reviews, vol. 111, pp. 3828-3857, 2011.

[6] M. Garcia, "Surface plasmons in metallic nanoparticles: fundamentals and applications," Journal of Physics D: Applied Physics, vol. 44, p. 283001, 2011.

[7] E. Kazuma and T. Tatsuma, "Localized surface plasmon resonance sensors based on wavelength-tunable spectral dips," Nanoscale, vol. 6, pp. 2397-2405, 2014.

[8] J. M. Bingham, J. N. Anker, L. E. Kreno, and R. P. Van Duyne, "Gas sensing with high-resolution localized surface plasmon resonance spectroscopy," Journal of the American Chemical Society, vol. 132, pp. 17358-17359, 2010.

[9] C.-S. Cheng, Y.-Q. Chen, and C.-J. Lu, "Organic vapour sensing using localized surface plasmon resonance spectrum of metallic nanoparticles self assemble monolayer," Talanta, vol. 73, pp. 358-365, 2007.

[10] G. Mie, "Beiträge zur Optik trüber Medien, speziell kolloidaler Metallösungen," Annalen der physik, vol. 330, pp. 377-445, 1908.
S. Murphy, L. Huang, and P. V. Kamat, "Reduced graphene oxide–silver nanoparticle composite as an active SERS material," The Journal of Physical Chemistry C, vol. 117, pp. 4740-4747, 2013.

[11] S. Iravani, H. Korbekandi, S. Mirmohammadi, and B. Zolfaghari, "Synthesis of silver nanoparticles: chemical, physical and biological methods," Research in pharmaceutical sciences, vol. 9, p. 385, 2014.

[12] K. Mavani and M. Shah, "Synthesis of silver nanoparticles by using sodium borohydride as a reducing agent," International Journal of Engineering Research & Technology, vol. 2, 2013.

[13] M. Cittadini, M. Bersani, F. Perrozzi, L. Ottaviano, W. Wlodarski, and A. Martucci, "Graphene oxide coupled with gold nanoparticles for localized surface plasmon resonance based gas sensor," Carbon, vol. 69, pp. 452-459, 2014.

[14] W. Jasinski and J. Berry, "Measurement of refractive indices of air, nitrogen, oxygen, carbon dioxide and water vapour at 3360 Mc/s," Proceedings of the IEE-Part III: Radio and Communication Engineering, vol. 101, pp. 337-343, 1954.

[15] Y. Clergent, C. Durou, and M. Laurens, "Refractive index variations for argon, nitrogen, and carbon dioxide at λ= 632.8 nm (He-Ne laser light) in the range 288.15 K≤ T≤ 323.15 K, 0< p< 110 kPa," Journal of Chemical & Engineering Data, vol. 44, pp. 197-199, 1999.